

UNCLASSIFIED

AD 404 542

*Reproduced
by the*

DEFENSE DOCUMENTATION CENTER

FOR

SCIENTIFIC AND TECHNICAL INFORMATION

CAMERON STATION, ALEXANDRIA, VIRGINIA



UNCLASSIFIED

NOTICE: When government or other drawings, specifications or other data are used for any purpose other than in connection with a definitely related government procurement operation, the U. S. Government thereby incurs no responsibility, nor any obligation whatsoever; and the fact that the Government may have formulated, furnished, or in any way supplied the said drawings, specifications, or other data is not to be regarded by implication or otherwise as in any manner licensing the holder or any other person or corporation, or conveying any rights or permission to manufacture, use or sell any patented invention that may in any way be related thereto.

404 542

806676

GENERAL APPLIED SCIENCE LABORATORIES, INC.

PAGE 1

(4) NA (5) 350320

Total No. Pages: 1 & 45

Copy No. () of ()

(7) 8 + (9) NA

(12) 45p. (13) NA

(14) TR-145A

(15) NA

(16) (17) (18) +

(19) NA

(20) 4

(21) NA

AD NO. — 404542

ASTIA FILE COPY

Fd

Scale 9

(6) FLUID MECHANICS OF
AXISYMMETRIC WAKES
BEHIND BODIES IN
HYPERSONIC FLOW

TECHNICAL REPORT NO. 145A

10
J. L. Ling and Paul A. Libby

Subcontract No. 214-361018

Prepared for

General Electric Company
Missile and Space Vehicle Department
Philadelphia, Pennsylvania

Prepared by

General Applied Science Laboratories, Inc.
Merrick and Stewart Avenues
Westbury, L.I., New York

June 1960

Approved by

Antonio Ferri
Technical Director

NO OTS

61-08-5331

**Best
Available
Copy**


TABLE OF CONTENTS

<u>Section</u>	<u>Title</u>	<u>Page</u>
	Summary	1
	Symbols	2
I	Introduction	5
II	Initial Conditions for the Shock-Induced Wake	9
III	Analysis of Flow in the Shock-Induced Wake	11
IV	Electron Concentration in a Laminar, Shock-Induced Wake	23
V	Electron Concentration in a Turbulent, Shock-Induced Wake	24
VI	Analysis for Boundary Layer Induced Wake	25
VII	Numerical Example of Boundary Layer Induced Wake	26
VIII	Concluding Remarks	31
	References	33
Appendix	Transformation of the Turbulent Compressible Wake Flow	34
	Figures	37

FLUID MECHANICS OF AXISYMMETRIC WAKES
BEHIND BODIES IN HYPERSONIC FLOW

By Lu Ting and Paul A. Libby

SUMMARY.

In this report ~~an~~ analysis of the fluid mechanics of wakes behind bodies in hypersonic flow is presented. The models used for idealizing both the flow field and the chemistry of air are discussed first. The fluid mechanics of the wake itself is then shown to be describable in terms of transformed coordinates which are applicable to both laminar and turbulent wakes. The transformation to the physical plane requires description of the transport properties of the gas; these are therefore discussed next. In this connection a rational means for estimating the turbulent transport properties is described. Finally, there are presented the results of numerical analysis of four cases which appear to lead to the highest concentration of electrons in the wake, and of the initial conditions for a boundary layer induced wake. 

SYMBOLS

a	amplitude of the velocity distribution as appears in Equation (14)
b	amplitude of mass fraction distribution
d	distance of the cross section of the wake from the body
D	base diameter of the body
$f(\eta)$	transformed stream function
h	static enthalpy; $h = 0$ at $^{\circ}\text{K}$
$\bar{h}, \bar{n}, \bar{p}, \bar{\mu}$	dimensionless quantities with respect to free stream conditions
H	total enthalpy including mean kinetic energy
Le	Lewis number
M	Mach number
n_e	electron density
p	pressure
Pr	Prandtl number
Re	Reynolds number
R_0	nose radius
\tilde{s}	transformed coordinate along body surface after Lee's theory
T	temperature
u, v	velocity components respectively in the axial and in the radial directions
u_{∞}	free stream velocity
W	molecular weight
r	cylindrical coordinates
$\tilde{x}, \tilde{r}, \tilde{b}$	dimensionless quantities with respect to the radius of the initial section of the incompressible wake

Y	mass fraction
z	incompressible radial coordinate as defined in Equation (8a)
γ	ratio of specific heats, $\frac{c_p}{c_v}$
δ	radius of the compressible wake
δ'	radius of the incompressible wake as defined in Equation (8e)
ϵ	absolute incompressible eddy viscosity as defined in Equation (29)
η	dimensionless variable as defined in Equation (8b)
θ	momentum thickness
Λ	$1 - a$
μ	absolute viscosity
μ_t	absolute eddy viscosity as defined in Equation (28)
ξ	dimensionless variable as defined in Equation (12)
ρ	density
ψ	stream function

Subscripts

∞	free stream conditions
e	quantities at the outer edge of the boundary layer
f	frozen flow
i	species i
j	atoms of species j
k	molecules of species k
o	conditions on the plane $x = 0$
s	stagnation conditions

Superscripts $\overline{(\quad)}$

time averages of fluctuating terms

*

transformed quantities referred to turbulent incompressible wake

I INTRODUCTION

The flow field behind a body in hypersonic flow can be divided into a region close to the body and a far field remote from the body. In the former region, the pressure is significantly different from its ambient value and is non-uniform in both the radial and axial directions. Moreover, in this region the viscous effects associated with base mixing play an important role in determining the flow field. The extent of this region close to the body can be estimated by application of the blast theory of S. C. Lin (Reference 1); if it is required that $p \geq 1.1 p_\infty$, with $M_\infty \approx 2.2$, $\gamma = 1.4$, then $x/D \approx 0.0665 M_\infty^2 \left[p/p_\infty - 0.405 \right]^{-1} \approx 46$; if $p/p_\infty \approx 1$ then $x/D \approx 54$. For the purpose of the wake these values of x/D correspond to "close" to the body.

The present analysis is concerned with the far field where viscous stresses predominate. The static pressure in this region is taken to be constant and equal to its ambient value. Therefore, the wake is being considered here as a generalization of the classical wake behind bodies in low speed flow.* In contrast to the low speed case, however, the hypersonic wake can involve changes across the viscous region of stagnation enthalpy, composition, and density as well as of velocity.

There appear to be two types of wake in the case of hypersonic flow. For blunt bodies the alterations in flow and gas properties from their free

*This problem is reviewed in Reference 2.

stream values are associated almost entirely with the bow shock wave and to a lesser degree with the shock wave system near the base of the body. The mass flow influenced by these shock waves is much greater than that involved in the boundary layer and base mixing. Thus the lateral extent of the portion of the wake caused by the boundary layer and base mixing is relatively small. The wake in this case can be idealized as a constant energy region with initial flow properties determined by the shock wave system. For slender bodies, on the contrary, the wake can be considered to be entirely due to the viscous effects associated with the boundary layer and base mixing. Then the energy is non-uniform across the wake.

The classification of hypersonic wakes then involves both shock-induced and boundary layer-induced wakes. In addition, it is possible to consider two different forms of transport corresponding to laminar and turbulent flow. Finally, assumptions concerning the chemical and thermodynamic behavior of the gas introduce an additional parameter. A realistic and complete description of the behavior of air is complex. In most analyses of fluid mechanical problems, it is customary to consider initially certain limiting cases of gas behavior. In the analysis described here, the composition of air is idealized into molecules, atoms and ions with the ions treated as having a molecular weight equal to that of the molecules. The electrons are taken to be equal in number to the number of ions and to be negligible from the fluid mechanical point of view. Finally, the ion concentration, while of interest, is assumed small so that the flow properties in the wake are determined by the molecules and atoms.

With this tertiary mixture as a model, there are various limiting cases of chemical and thermodynamical behavior to be considered. The usual cases of complete equilibrium and completely frozen composition are supplemented by several others. For example, the concentration of molecules and atoms can be considered to be frozen; from the flow analysis, a "state" defined by a pressure and temperature can be found. The concentration of ions in this state can be assumed to be given by equilibrium air in that state. Such a case corresponds to frozen dissociation and equilibrium ionization. A fourth limit clearly corresponds to equilibrium dissociation and frozen ionization.

Thus the two forms of wake, the two transport mechanisms and the four limiting cases of gas behavior result in 16 different types of wake which can be analyzed in terms of the idealizations discussed here. The analysis of the wake which is presented below is applicable to all of these cases; it is based on the application of integral methods to wake flow due to Bloom and Steiger (Reference 3). There result relatively simple expressions for the flow properties in the wake in terms of transformed coordinates, of the gas properties along the axis of the wake, and of conditions at the origin of the wake. The application of these expressions to a particular wake flow, therefore, involves the determination of the gas properties and of the initial conditions for the wake and then the evaluation

of the inverse transformation to obtain the flow parameters in the physical plane

Primary emphasis has been devoted here to those cases which would appear to lead to the highest concentration of electrons in the wake. Preliminary analyses indicated that the shock-induced wake with complete equilibrium and with completely frozen composition were thus to be emphasized; therefore, attention is directed to the four cases which so arise. The theoretical analysis of the boundary layer induced wake is also presented along with a numerical analysis of the initial conditions in such a wake. In the following section, the initial conditions for the shock-induced wake are discussed.

The authors are pleased to acknowledge the helpful suggestions of Dr. Antonio Ferri and Dr. M. H. Bloom concerning the analysis presented here and the assistance of Mr. Paul Baronti in the numerical analysis.

II INITIAL CONDITIONS FOR THE SHOCK-INDUCED WAKE

The major contribution to the wake behind a blunt body in hypersonic flow arises from the bow shock. It is therefore assumed that the bow shock shape is given and that the initial conditions for the wake are derived. In accordance with the idealizations described above, these initial conditions involve the radial distributions of the axial velocity, of the concentrations of molecules, atoms and ions, and of a state variable, for example, temperature. The static pressure throughout the wake is assumed constant and known.

From the shock shape and the tables of Feldman (Reference 4), the state of the mixture at each point behind the shock can be found for a given flight velocity and altitude. These mixture properties can be used in conjunction with the equilibrium compositions tabulated by Logan (Reference 5) to determine completely the state of the air behind the shock. An assumption must be made concerning the thermodynamic and chemical process experienced by the gas in going from its state behind the shock to the ambient pressure p_{∞} . For the calculations herein reported, two isentropic processes were considered corresponding to complete equilibrium and completely frozen flow. With these assumptions, the state of the flow (velocity, composition and temperature) where the static pressure is p_{∞} can be determined for each streamline originating at the shockwave. There remains only the determination of the radial positions of the streamlines.

This can be done by a streamtube method of analysis involving application of the condition of mass conservation starting from the axis of symmetry. For the case of frozen composition the tables of Huff et al in Reference 6 were used in conjunction with the composition data from Reference 5.

The body considered for numerical analysis according to this method is the 7.10 configuration with a base radius of one foot assumed. There was available a schlieren photograph of the shock shape at a Mach number of 6.0 (Reference 7). By application of the Mach number independence principle this same shape was used to determine the initial values for the wake corresponding to a velocity of 23,200 ft/sec at an altitude of 200,000 feet. The results for the initial distributions according to the two aerodynamic processes are shown in Figures 1 to 4. It should be noted that if the radial distributions for a base radius of the body equal to 2.5 feet are desired, then ϕ_0 and the radial scale associated with x and r must be multiplied by 2.5; that is, the wake is 2.5 times greater in diameter.

III ANALYSIS OF FLOW IN THE SHOCK-INDUCED WAKE

We assume that the wake begins at a plane $x = 0$ which is at distance d_0 behind the body. On the initial plane $x = 0$, all the flow properties are prescribed, for example, as shown in Figures 1 to 4. The problem is to study how the flow in the wake approaches the uniform flow outside the wake for the case of shock-induced wake.

Since the length of wake is much larger than the diameter of the cross-section, the usual boundary layer assumption is applicable. The pressure, p , across the wake is constant and is equal to that of the surrounding uniform flow, i.e.,

$$p = p_{\infty} \quad (1)$$

With the assumption that the Prandtl number Pr and the Lewis number Le are equal to unity, the energy equation for shock-induced wake is fulfilled by the Crocco integral

$$h + \frac{u^2}{2} = h_{se} = \text{const.} \quad (2)$$

The assumptions concerning the Prandtl and Lewis numbers are not necessary when we employ the integral method in which the differential equations are replaced by the integral equations or the conservation laws across the entire wake layer. This argument will be substantiated in the treatment of frozen flow.

The continuity and momentum equations for the wake flow are

$$\frac{\partial(\rho u r)}{\partial x} + \frac{\partial(\rho v r)}{\partial r} = 0 \quad (3)$$

and

$$\rho u r \frac{du}{dx} + \rho v r \frac{dv}{dr} = \frac{d}{dr} \left(\mu r \frac{du}{dr} \right) \quad (4)$$

These equations are applicable for laminar flow and also for turbulent flow if eddy viscosity is introduced in place of the viscosity coefficient μ . In the following analysis it should be understood that the symbol μ denotes either the laminar or turbulent transport coefficient. When the integral method is employed, these two differential equations for u and v are replaced by the integral relationship for u :

$$\frac{d}{dx} \int_0^{\delta} \rho u r (u_{\infty} - u) dr = 0$$

where $\delta(x)$ is the radius of the wake region. This equation states that the total momentum is conserved in the wake region and that the momentum thickness θ is a constant (References 2 and 3). Thus

$$\theta = \frac{1}{\rho_{\infty} u_{\infty}^2 \delta_0'} \int_0^{\delta(x)} \rho u r (u_{\infty} - u) dr = \frac{1}{\rho_{\infty} u_{\infty}^2 \delta_0'} \int_0^{\delta_0} \left[\rho u r (u_{\infty} - u) \right] \Big|_{x=0} dr = \text{const } \theta_0 \quad (5)$$

where $\delta(x)$ is the radius of the wake and δ_0' is the associated incompressible wake radius at $x = 0$ as defined in Equation (8c).

The boundary conditions for u are

$$\text{at } r = \delta, \quad u/u_{\infty} = 1, \quad \frac{\partial u}{\partial r} = 0 \quad (6a, b)$$

$$\text{and at } r = 0, \frac{\partial u}{\partial r} = 0 \text{ and } \rho u \frac{\partial u}{\partial x} = 2\mu \frac{\partial^2 u}{\partial r^2} \quad (7a, b)$$

The last boundary condition is obtained from Equation (4) (cf. Reference 8).

The compressible wake is transformed into an associated incompressible wake by the transformation (Reference 8)

$$z^2 = \int_0^r \tilde{\rho} \, dr^2 \quad (8a)$$

which in turn is transformed to the dimensionless variable η ,

$$\eta = z \delta' \quad (8b)$$

$$\text{where } \tilde{\rho} = \rho/\rho_\infty, (\delta')^2 = \int_0^{\delta^2} \rho \, dr^2 \quad (8c)$$

Equations (5), (6) and (7) then become

$$\frac{\partial \bar{\theta}}{\partial \eta} = \tilde{\delta}^2 \int_0^1 \eta \tilde{u} (1 - \tilde{u}) \, d\eta \quad (9)$$

$$\tilde{u} = 1, \frac{\partial \tilde{u}}{\partial \eta} = 0 \text{ at } \eta = 1 \quad (10a, b)$$

$$\frac{\partial \tilde{u}}{\partial \eta} = 0 \text{ and } \tilde{u} \frac{\partial \tilde{u}}{\partial \tilde{x}} = \frac{2}{Re} \frac{\tilde{u}}{(\tilde{\delta})^2} \frac{\partial^2 \tilde{u}}{\partial \eta^2} \text{ at } \eta = 0 \quad (11a, b)$$

where $\tilde{\delta} = \delta'/\delta'_0$, $\tilde{u} = u/u_\infty$, $\tilde{\mu} = \mu/\mu_\infty$, $\tilde{x} = x/\delta'_0$ and $Re = \rho_\infty u_\infty \delta'_0 / \mu_\infty$

Moreover, if we transform \tilde{x} into ξ by the relationship

$$\frac{1}{Re} \int_0^{\tilde{x}} \tilde{\mu} [\tilde{x}, \eta = 0] \, d\tilde{x} = \xi \quad (12)$$

The last boundary condition becomes

$$\bar{u} \frac{\partial \bar{u}}{\partial \xi} = \frac{2}{(\bar{\delta})^2} \frac{\partial^2 \bar{u}}{\partial \eta^2} \quad \text{at } \eta = 0 \quad (13)$$

Equations (9), (10a,b), (11a) and (13) are explicitly independent of $\bar{\rho}$ and $\bar{\mu}$. Therefore, we can solve for \bar{u} as a function of ξ , η fulfilling Equation (9) and boundary conditions (10a, b), (11a) and (13) and also the initial data at $\xi = \bar{x} = 0$. The effect of $\bar{\rho}$ and $\bar{\mu}$ enters the problem through the initial data; through the values of δ_0 and θ , and through the inverse transformation from the ξ , η plane to the physical plane of x , r .

If the initial profile for \bar{u} , which also fulfills the boundary conditions Equations (10a,b) and (11a), can be approximated by a third order polynomial in η as

$$u(\xi = 0, \eta) = 1 - (1 - a_0)(1 - 3\eta^2 + 2\eta^3) \quad (14)$$

$$\text{or} \quad 1 - \bar{u}(0, \eta) = (1 - a_0)(1 - \eta)^2(1 + 2\eta)$$

then, the velocity profile in the wake can be expressed as

$$1 - \bar{u}(\xi, \eta) = [1 - a(\xi)] (1 - \eta)^2(1 + 2\eta) \quad (15)$$

which obviously fulfills the conditions of Equations (10a,b) and (11a).

Consider now the approximation of the initial velocity data of Figures 1 and 2 obtained with Equation (14). To make a comparison it is necessary to evaluate $u(0,0)$ and δ_0 . This was done by application of the method of least squares. The resulting curves of $1 - u(0, \eta) u_{\infty}$ versus z are shown in Figures 1 and 2. It will be noted that rough quantitative agreement is obtained. If a more exact representation of the initial profile is desired,

additional coefficients must be introduced into Equation (14); these must be treated as functions of ξ with the requisite additional equations determined either from additional boundary conditions at $r = 0$ or from the momentum equation multiplied by u or r and integrated with respect to r . For the purposes of the present analysis the degree of approximation achieved by Equation (14) is considered satisfactory. Equations (9) and (13) yield, respectively:

$$\frac{\theta}{\delta_0^2} = \delta^2 \left[0.15(1-a) - 0.0857(1-a)^2 \right] \quad (16)$$

$$= 0.15(1-a_0) - 0.0857(1-a_0)^2 = \frac{\theta}{\delta_0^2}$$

and
$$a \frac{da}{d\xi} = (12) \frac{1-a}{\delta^2} \quad (17)$$

Elimination of δ yields

$$\frac{a\theta_0}{\delta_0^2} \frac{da}{d\xi} = 12(1-a)^2 \left[0.15 - 0.0857(1-a) \right]$$

By integration, ξ is expressed in terms of Λ or $1-a(\xi)$,

$$\xi = \frac{\theta_0}{\delta_0^2} \left\{ 0.5556 \left(\frac{1}{\Lambda} - \frac{1}{\Lambda_0} \right) - 0.2381 \log_e \frac{\Lambda_0 (1.75 - \Lambda_0)}{\Lambda (1.75 - \Lambda)} \right\}$$

where $\Lambda_0 = 1 - a_0$.

Equations (2), (14) and (18) give the velocity and static enthalpy distributions in the $\xi - \eta$ plane, valid for either equilibrium or frozen flow and for either laminar or turbulent flow. These cases require separate treatment in the determination of the transformation from the ξ, η

plane to the physical plane x, r , of the transport properties and the electron density, and of the initial values.

Consider now the four cases corresponding to laminar and turbulent flow and to complete equilibrium and to completely frozen concentration.

(A) Equilibrium Laminar Flow

Corresponding to each point ξ, η the static enthalpy h is obtained from Equation (2) with the velocity u given by Equations (18) and (14). With $p = p_\infty$, the state of the fluid, the electron density n_e , and the viscosity are known for each value of h .

At each station of x or ξ , n_e is maximum on the ξ -axis. The distribution of $n_e(\xi, 0)$ with respect to x is obtained from the inverse transformation of Equation (12),

$$x = \delta'_0 R_e \int_0^\xi \left[\bar{\mu}(\xi, 0) \right]^{-1} d\xi \quad (19)$$

which is carried out by numerical integration.

(B) Frozen Laminar Flow

In this limiting case, we assume that the volume recombination rates within the wake are low compared to diffusion across streamlines. The mixture in the wake in general is composed of molecules O_2, N_2, NO ; atoms O, N and electrons and the associated ionized molecules and atoms. The number of the ionized particles per cubic centimeter is large (on the order of 10^{12} for the conditions selected for numerical analysis), yet it is

small compared to the total number of particles per cubic centimeter.

Thus to a satisfactory degree of approximation the effect of ionized particles can be neglected in the determination of the states of the mixture.

If Y represents the mass fraction of species i in the wake, the continuity equation for this specie according to the integral method becomes the law of conservation of mass for each species in the wake region, that is,

$$\frac{d}{dx} \int_0^{\delta} \rho u (Y_{i\infty} - Y_i) dr = 0$$

Since $Y_{i\infty} = 0$ for atoms and $Y_{i\infty} \neq 0$ for molecules this equation after transformation from r to η becomes:

$$(\delta^*)^2 \int_0^1 \eta \cdot Y_j d\eta = \text{const.} \quad \text{subscript } j \text{ for atoms} \quad (20a)$$

and

$$(\delta^*)^2 \int_0^1 \eta u (1 - Y_k / Y_{k\infty}) d\eta = \text{const.} \quad \text{subscript } k \text{ for molecules} \quad (20b)$$

The boundary conditions are

at $\eta = 1$, $Y_j = 0$, $\frac{\partial Y_j}{\partial \eta} = 0$, $Y_k / Y_{k\infty} = 1$, $\frac{\partial Y_k}{\partial \eta} = 0$ (21a)

and at $\eta = 0$, $\frac{\partial Y_j}{\partial \eta} = 0$, $\frac{\partial Y_k}{\partial \eta} = 0$ (21b)

If Y_j is represented by a third order polynomial of η , the boundary conditions of Equations (21a, b) result in the dependence of Y_j on η identical

*It should be noted that this law prevails independent of the relation between diffusional velocities and concentration gradients.

to the dependence of $1 - u/u_\infty$ on η , i.e.,

$$Y_j = b_j(\xi) (1-\eta)^2 (1+2\eta) = \frac{b_j(\xi)}{1-a(\xi)} \left(1 - \frac{u}{u_\infty}\right)$$

Equation (20a) then becomes

$$\frac{(b_j')^2 b_j(\xi)}{1-a(\xi)} \int_0^1 \eta u \left(1 - \frac{u}{u_\infty}\right) d\eta = \text{const.}$$

From Equation (9) it is clear that the above leads to

$$\frac{b_j(\xi)}{b_j(0)} = \frac{1-a(\xi)}{1-a(0)}$$

or

$$\frac{Y_j(\xi, \eta)}{Y_j(0, 0)} = \frac{u_\infty - u(\xi, \eta)}{u_\infty - u(0, 0)} \quad (22a)$$

Similarly, if $Y_k/Y_{k\infty}$ is represented by a third order polynomial in η , the dependence of $1 - Y_k/Y_{k\infty}$ on η will be identical to that of $1 - u/u_\infty$, i.e.,

$$\frac{Y_{k\infty} - Y_k(\xi, \eta)}{Y_{k\infty} - Y_k(0, 0)} = \frac{u_\infty - u(\xi, \eta)}{u_\infty - u(0, 0)} \quad (22b)$$

It is of interest to reconsider at this point the assumptions with respect to the Prandtl and Lewis numbers. In the species conservation the assumption of a polynomial profile for Y_i of the same degree as the velocity profile leads to Equation (22). However, if an additional coefficient resulting in a fifth degree polynomial for Y_i is assumed, and accordingly an additional boundary condition at $\bar{r} = 0$ is imposed, there will result a

differential equation analogous to Equation (17) for the determination of this extra coefficient as a function of ξ . In this case the diffusion coefficient D_{12} evaluated at the axis will arise. In an analogous fashion a stagnation enthalpy profile could be assumed as a substitute for the Crocco integral Equation (2). The additional coefficient in this profile would be determined by a corresponding boundary condition at $\bar{r} = 0$ arising from the energy equation. In this case the Prandtl and Lewis numbers along the axis of the wake would arise. The initial values of the additional coefficients would be selected so that the initial profiles would be more closely approximated than is possible with the profiles used here.

Knowing $Y_j(\xi, \eta)$ and $Y_k(\xi, \eta)$, we can compute the density of the mixture $\bar{\rho}$. The temperature of the mixture is determined such that the static enthalpy \bar{h} of the mixture agrees with that from Equation (2).

Because of the close similarity between the transport properties and the atomic weights of oxygen and nitrogen, the transport properties of the mixture in the wake will be calculated by the formula for a binary mixture of atoms and molecules according to the suggestion of Penner (Reference 9). The transport properties of binary mixture are obtained from the following formulas (cf. Reference 10, for example):

$$\mu_i = 2.67 \times 10^{-5} \frac{\sqrt{W_i T}}{\sigma_i^2 \Omega_i^{(2,2)*}(T_i)^*}, \quad i = 1, 2$$

$$\mu_{\text{mix.}} = \frac{X_1^2}{\mu_1 + \left[\frac{1.385 X_1 X_2 R T}{(p_{\infty} W_1 D_{12})} \right]} + \frac{X_2^2}{\mu_2 + \left[\frac{1.38 X_1 X_2 R T}{(p_{\infty} W_1 D_{12})} \right]} \quad (23)$$

$$D_{12} = 2.628 \times 10^{-4} \frac{\left[T^3 (W_1 + W_2) / 2 W_1 W_2 \right]^{1/2}}{p_{\infty} D_{12}^{1/2} \Omega_{12} (1.1)^* (1.1)^*} \quad (24)$$

(The definitions and the units are the same as those given in Reference 10.)

The following constants have been used in the calculation (Reference 9):

$$\begin{aligned} W_1 &= 14.5 & W_2 &= 29 \\ U_1 &= 0.80 \text{ Å} & \epsilon_1/k &= 114 \text{ K} \\ U_{12} &= 3.3 \text{ Å} & \epsilon_{12}/k &= \epsilon_2/k = 84^\circ \text{ K} \\ U_2 &= 3.69 \text{ Å} \end{aligned} \quad (25)$$

If n_e denotes the number of electrons per cubic centimeter, then $n_e/\bar{\rho}$ is the number of electrons per unit mass of the mixture. The continuity equation for the electrons according to the integral method is the equivalent to the conservation of electrons in the wake, i.e.,

$$\frac{d}{dx} \int_0^{\delta} \bar{\rho} u r (n_e/\bar{\rho}) dr = 0 \quad (26)$$

This equation for $n_e/\bar{\rho}$ is the same as that for Y_1 and furthermore they have the same boundary condition, therefore, if $n_e/\bar{\rho}$ is represented by a third order

polynomial of η , the solution should be similar to that for Y_1 , i.e.,

$$\frac{n_e(\xi, \eta) \bar{\rho}(0, 0)}{n_e(0, 0) \bar{\rho}(\xi, \eta)} = \frac{u_\infty - u(\xi, \eta)}{u_\infty - u(0, 0)} \quad (27)$$

The inverse transformation from ξ, η to x, r plane can be accomplished by numerical integration since we know $\bar{\rho}(\xi, \eta)$ and $\mu_{\text{mix}}(\xi, \eta)$.

In Figure 3 there is shown the mass fraction of atoms given by Equation (22) with δ'_0 determined from the velocity profile (cf. figure 2), and with $Y_1(0, 0)$ determined by the method of least squares. In Figure 4 the ratio of the number of electrons per unit mass in the wake to the corresponding number at the axis as given by Equation (27) again with δ'_0 determined from the velocity profile and $n_e(0, 0)/\bar{\rho}(0, 0)$ determined by the method of least squares. For both of these profiles the same comments as were made previously for the velocity profiles are applicable.

(C) Turbulent Wake (Equilibrium or Frozen Flow)

In the ξ, η plane, the state in the wake is independent of μ , therefore, the results for equilibrium or frozen laminar wake flow can be employed for the corresponding turbulent flow provided that the symbol μ is interpreted as the absolute eddy viscosity μ_t instead of the absolute viscosity μ in the transformation from ξ - η plane to the physical x - r plane. Experimental data for absolute eddy viscosity for compressible wake flows do not appear to be available. Mager (Reference 11) has shown, however, that for boundary layer flows the compressible values of μ_t can be

correlated to the incompressible eddy viscosity ϵ^* . Mager's correlation can be modified (see Appendix) for the transformation of compressible axisymmetric wake flow; there results

$$\mu_t = \frac{\rho \omega \epsilon^*}{\bar{\rho} r^2} \int_0^{r^2} \bar{\rho} dr^2 \quad (28)$$

According to Reference 2, pages 492-501, the incompressible eddy viscosity ϵ^* for wakes and jets can be expressed as

$$\epsilon^* = 2k_1(\delta^*)_0 \left[u_{\infty} - u(0,0) \right] \quad (29)$$

where $(\delta^*)_0 = \delta_0^*$ is the radius of the corresponding incompressible wake at the initial station.

The value of k_1 ranges from 0.02 to 0.005 for mixing of two-dimensional or circular jets and for two-dimensional wakes. Since a different value of k amounts only to a different scale of x in the physical plane, the value of 0.01 considered typical will be employed in the present calculation. With μ replaced by μ_t the procedure developed for the laminar wake can be applied to the turbulent wake.

IV ELECTRON CONCENTRATION IN A LAMINAR, SHOCK-INDUCED WAKE

The transformations to the physical plane have presently been completed for the cases corresponding to cases A and B of the previous section. The results in terms of number of electrons per unit volume along the axis $n_e(0, x)$ are shown in Figure 5. It should be noted that the x scale therein corresponds to a base diameter of one foot; for a base diameter equal to 2.5 feet these dimensions should be multiplied by $(2.5)^2 = 6.25$.

For the case of equilibrium flow the results of Figure 5 indicate that the number of electrons per unit volume is relatively low at the initial station and decreases by a factor of two in roughly 24,000 feet for a body of base diameter 2.5 feet. For frozen ionization the number of electrons per unit volume is relatively high at the initial station (1.8×10^{12}) and decreases by a factor of two in 9,200 feet, again for a base diameter of 2.5 feet.

V ELECTRON CONCENTRATION IN A TURBULENT, SHOCK- INDUCED WAKE

Based upon the transformations in Section III C, the results in terms of number of electrons per unit volume along the axis $n_e(0, x)$ are shown in Figure 6 for both equilibrium flow and frozen flow.

As compared to the corresponding laminar cases in Figure 5, the length scale for the same decay in electron density is reduced by an order of 350 for the equilibrium flow and by an order of 250 for the frozen flow.

VI ANALYSIS FOR BOUNDARY LAYER INDUCED WAKE

The analysis for the case of boundary layer induced wake can be carried out along lines similar to that described above for the shock-induced wake. We consider as a first analysis the approximation of Prandtl number of unity. Then since the wake is treated as a constant pressure region, the Crocco integral given by Equation (2) can be extended so that

$$h + u^2/2 = A + B u \quad (30)$$

where A and B are constants determined by two conditions; the first is clearly that $h = h_{\infty}$ when $u = u_{\infty}$ while the second must be obtained from a specification of the total energy lost by the stream to the body generating the wake. Consider, therefore, that A and B are known.

The solution for the velocity distribution on the ξ, η plane given by Equations (14) and (18) is still valid for the case. However, the enthalpy distribution will now be obtained from Equation (30) rather than from Equation (2) and therefore will change. The transformation to the x, r plane obtained from the inverse of Equation (12) must also be carried out numerically and will be altered by the change in the velocity-enthalpy relation.

VII NUMERICAL EXAMPLE OF BOUNDARY LAYER INDUCED WAKE

In order to provide an indication of the wake associated with the boundary layer, the flow about a slender, spherically-capped cone is considered. The half-cone angle is taken to be 15° so that the ionization and dissociation behind the conical shock is negligible. Moreover, a base radius of 2.5 feet is assumed in order to permit comparison of this boundary layer induced wake with those computed above. Finally, the radius of the spherical cap is selected so that at the flight conditions corresponding to 200,000 feet the mass entering the boundary layer at base of the body has passed through the conical shock. The boundary layer is conservatively assumed to be laminar.*

In calculating the radius of the spherical cap the Levy-Lees transformation (cf. Reference 10) is applied along with the assumption of uniform external flow on the cone ($\beta \approx 0$). The mass entering the boundary layer at a station x measured along the surface of the body originates in a streamtube of radius r_∞ according to the following equation

$$\rho_\infty V_\infty \pi r_\infty^2 = 2\pi\psi = 2\pi\sqrt{2\tilde{s}} \, 1(\eta_e) \quad (31)$$

where the subscript ∞ denotes flight conditions, ψ is the stream function, \tilde{s} is the transformed x coordinate defined by the equation

$$\tilde{s} = \int_0^x \rho_e u_e r^2 dx$$

*Note that if the flow is turbulent, the streamline considered here will enter the boundary layer upstream of the base.

and finally where $f(\eta_c)$ is the value of the transformed stream-function evaluated at the "edge" of the boundary layer.* For $u/\eta_c \approx 0.994$, $f(\eta_c) \approx 2.5$.

It is sufficiently accurate for present purposes to neglect in the computation of $\tilde{s}^{1/2}$ the influence of the spherical cap which is expected to be of relatively small radius. Thus using a Newtonian pressure on the cone and the oblique shock properties given by Reference 4, we find r_∞ from Equation (31). There was available a shadowgraph obtained at a Mach number of 7.9 on a spherically-capped 15° half-angle cone. Employing Mach number independence principle, we can find the value of the nose radius such that the streamtube with the computed value of $r_\infty = (r_\infty)_f$ passes through the junction of the conical and curved portions of the bow shock. This nose radius is found to be 4.1 inches.

With the nose radius determined, the shadowgraph can be used in conjunction with the gas and flow tables of References 4 and 5 to determine the state and composition of the gas behind the shock and thus as a function of the radial position of the point in question on the shock. The mass fraction of the constituents considered are shown in Figure 7. These data are required for the determination of the initial condition in the wake analysis.

Consider next the thermodynamic process experienced by the gas in flowing from the region behind the shock, through the boundary layer and into the wake behind the body. The process leading to the greatest electron

*Note that if mass is injected into the boundary layer by mass transfer from the body, the value of $f(\eta_c)$ must be altered and the contribution of the injected gas to the initial composition of the wake must be considered.

population in the wake is as in the case of the shock-induced boundary layer that of completely frozen flow; thus for the subsequent analysis this conservative case will be considered.

We discuss first the initial profiles of velocity, density, temperature and composition in the wake where as above we take $p = p_\infty$. The velocity and stagnation enthalpy distributions at the trailing edge of the body are assumed to be given by flow on the cone ($\theta = 0$); in terms of the Levy-Lees transformations with the assumptions $\mu \propto p_e \mu_e$, and unity Prandtl number the Blasius values tabulated in Reference 2 and the Crocco integral can be employed. With the assumption of an isentropic expansion from the trailing edge of the cone to the pressure p_∞ , the velocity $u(0, 0)$ at the center of the initial cross section of the wake is obtained. At the edge of the wake $r = \delta_0$ or $z = \delta_0' u = u_\infty$ where δ_0' is the associated incompressible wake radius as defined in Equation (8c). With the assumption of a distribution of the velocity profile equivalent to Equation (15), i.e.,

$$\frac{u(0, \eta) - u(0, 0)}{u(0, 1) - u(0, 0)} = (1 - \eta)^2 (1 + 2\eta)$$

where $\eta = z/\delta_0'$, the initial wake radius δ_0' is determined by the condition of conservation of mass:

$$\rho_\infty (\delta_0')^2 \int_0^1 u(0, \eta) \eta d\eta = \int_0^{\delta_0} \rho u r dr = \rho_\infty u_\infty r_\infty^2$$

It will be noted that the initial radius δ_0' is 1.04 feet as compared to 9.75 feet in the case of the shock induced wake for a body of 2.5 feet base radius.

The further determination of the gas composition is more complex. Consideration of the mass fractions of constituents shown in Figure 7 indicates that no simple polynomial expressions can be employed to approximate the relations between mass flow and mass fraction, for the purpose of estimating the initial state of the wake, straight-line segments were employed along with the requirements of species conservation corresponding to frozen flow; this requirement can be expressed as

$$\left(\rho_w u_w \int_0^{(r_w)_f} Y_i u dr \right)_{\text{shock}} = \left(\int_0^{\delta_w} \rho Y_i u dr \right)_{x=0 \text{ in wake}} \quad (32)$$

The left hand side of Equation (32) can be evaluated for each i from Figure 7, while for the right hand side it is convenient to use the transformed variable η in place of r , thus from Equation (8a)

$$\left(\int_0^{\delta_w} \rho Y_i u dr \right)_{x=0 \text{ in wake}} = \frac{\rho_{\infty} (\delta_w^*)^2}{2} \left(\int_0^1 Y_i u d\eta \right)_{x=0 \text{ in wake}} \quad (33)$$

Provided straight line segments for $Y_i = Y_i(\eta)$ are assumed the distributions of the mass fractions of the main constituents shown in Figure 8 are obtained.

We are now able to find the density and temperature distributions corresponding to the pressure p_{∞} and to the static enthalpy distribution which is given by the Crocco relationship since

$$\rho = \rho(z) = \frac{p_{\infty}}{R T(z) \sum \frac{Y_i(z)}{W_i}} \quad (34)$$

while $Y(z)$ is given parametrically by the equation

$$h = h(z) = \sum h_i(T) Y_i(z) \quad (35)$$

The distribution of ρ/ρ_∞ vs. η is shown in Figure 9.

In order to estimate the electron distribution, it will be approximated by a third order polynomial of η , i.e.,

$$n_e(0, \eta) = n_e(0, 0)(1 - \eta)^2(1 + 2\eta)$$

due to the boundary conditions at $\eta = 1$ and $\eta = 0$.

The amplitude $n_e(0, 0)$ is determined by the condition of conservation total electron population from the shock to the wake, i.e.,

$$\int_0^{r_\infty} n_e r_\infty dr_\infty = (\delta_0^*)^2 \int_0^1 n_e(0, \eta) \left(\frac{1}{p}\right) \eta d\eta$$

This condition yields a higher estimate because of the loss of electrons in the stream tubes near the surface of the cone.

The value of $n_e(0, 0)$ is 1.21×10^{10} electrons per c.c. This value is $1/19$ of that for a shock induced wake. The initial radius is approximately $1/9.4$ times that in the shock induced wake. The decay of electron density can be estimated from that in a shock induced wake with the length scale along the x-axis reduced by a factor $(1/9.4)^2$. For example, the electron density will decrease from 1.21×10^{10} to 6×10^{10} in a distance of 100 feet.

VIII CONCLUDING REMARKS

An analysis of the fluid mechanical aspects of the wakes behind bodies in hypersonic flow has been carried out. The flow has been idealized so that the pressure is constant and the boundary layer approximations are valid. Both laminar and turbulent flows are considered. Furthermore, two limiting cases are considered corresponding to the shock-induced wake and to the boundary layer induced wake. The main interest in this study is the electron concentration in the wake. Preliminary analysis indicated that the greatest number of electrons would arise from the cases of complete equilibrium flow or completely frozen flow, therefore, the chemical and thermodynamic behavior of the gas is idealized in two different ways corresponding to these two cases.

By appropriate transformations the velocity distribution in a transformed plane can be obtained for all cases of laminar or turbulent flow, shock- or boundary layer-induced wake, frozen or equilibrium gas behavior. The inverse transformation to the physical plane differs in each case and must be performed numerically.

Numerical results have been obtained for laminar and turbulent flow with a shock-induced wake corresponding to the 3.10 configuration. The flight conditions were taken to be 23,200 fps and 200,000 feet altitude. Although the detailed calculations were carried out for a base radius of one foot, the scaling to a base radius of 2.5 feet is easily performed. The case of equilibrium, laminar flow is found to yield an electron concentration at the

origin of the wake of roughly 2×10^{10} electrons/cc. This concentration decays by a factor of two in a length of 24,000 feet for a body with base diameter of 2.5 feet. For frozen flow the electron concentration is approximately 1.8×10^{12} /cc at the origin of the wake and decays to one-half in a length of 9,000 feet for a body of the same base radius. For the corresponding turbulent cases, the scale of length is reduced from the laminar values by roughly 350 for equilibrium flow and by 250 for frozen flow.

As an indication of the wake associated with the boundary layer, the flow about a slender spherically capped cone is considered. The half cone angle is 15° , the base radius is 2.5 feet and the nose radius of 4.1 inches is chosen so that the fluid passing through the curved position of the bow shock just completed is swallowed by the boundary layer at the trailing edge of the cone. The maximum electron density at the initial cross-section of the wake is roughly 1.2×10^{12} per c.c. It is one-fifteenth of the corresponding value in the shock-induced wake corresponding to the 3, 10 configuration and decays to one-half in a distance of 100 feet.

REFERENCES

1. Lin, S. C., "Cylindrical Shock Waves Produced by Instantaneous Energy Release", Journal of Applied Physics, Vol. 25, pp. 54-57, 1954.
2. Schlichting, H., "Boundary Layer Theory", McGraw-Hill Book Co., Inc., 1955.
3. Bloom, M. H. and Steiger, M., "Viscous Reacting Wake Flow: Symmetric and Asymmetric", PIBAL Report No. 544, Polytechnic Institute of Brooklyn.
4. Feldman, Saul, "Hypersonic Gas Dynamic Charts for Equilibrium Air", AVCO Research Laboratory, January 1957.
5. Logan, J. G., Jr., "Thermodynamic Charts for High Temperature Air Calculations (2000°K to 9000°K)", Cornell Aeronautical Laboratory Report No. AD-1052-A-4, July 1956.
6. Huff, Vearl N., Gordon, Sanford and Morrell, Virginia E., "General Method of Thermodynamic Tables for Computation of Equilibrium Composition and Temperature of Chemical Reactions", NACA Report 1057, 1951.
7. Bloom, M. H. and Pallone, A., "Pressures and Heat Transfer Rates Over a Blunt-Nosed Body Tested at Mach 6.0", GASL Technical Report No. 47, December 1957 (Report Secret- Title Unclassified).
8. Pai, S. I., "Axially-Symmetrical Jet Mixing of a Compressible Fluid", Quarterly of Applied Mathematics, Vol. X, No. 2, pp. 141-148, July 1952.
9. Penner, S. S., "Chemistry Problems in Jet Propulsion", Pergamon Press, New York, 1957.
10. Lees, L., "Laminar Heat Transfer Over Blunt-Nosed Bodies at Hypersonic Flight Speeds", Jet Propulsion, pp. 259-269, April 1956.
11. Mager, A., "Transformation of the Compressible Turbulent Boundary Layer", Journal of the Aeronautical Sciences, Vol. 25, No. 5, pp. 305-311, May 1958.

APPENDIX *TRANSFORMATION OF THE TURBULENTCOMPRESSIBLE WAKE FLOW

The governing equations for axisymmetric turbulent wake flow are:

$$(\rho ur)_x + (\rho vr + \overline{\rho'v'r})_r = 0 \quad (A-1)$$

$$r\rho u u_x + (\rho vr + \overline{\rho'v'r})u_r - (\rho r u'v')_r \quad (A-2)$$

$$\rho ur H_x + (\rho vr + \overline{\rho'v'r})H_r - (\rho r v'H')_r \quad (A-3)$$

We have already employed two assumptions that the pressure is nearly constant in the wake and the effects of viscosity and conductivity can be neglected.

In these equations the primes denote the fluctuating terms and H , the total enthalpy, includes the mean kinetic energy. Equation (A-3) is fulfilled by the solution $H = \text{constant}$ and $\overline{v'H'} = 0$.

In addition to the requirement in the laminar flow transformation that the stream function remains unchanged, we impose on the transformation the following conditions:

- a. The reference conditions at the free stream value should be used.
- b. The moment of the turbulent shear about the axis is constant over an infinitesimal mass of the fluid.

Condition (a) is more appropriate for wake flow than Mager's which was introduced for boundary layer flow.

*A note based on this appendix has been accepted for publication in the Journal of the Aero/Space Sciences.

Condition (b) is also different from Mager's because of the appearance of the moment of stress $\rho \bar{u'v'}$ in the equation of motion.

With ()^{*} indicating the quantities in the transformed system the transformations are

$$\rho^* = \rho_{\infty} \quad (A-4)$$

$$x^* = x \quad (A-5)$$

$$(r^*)^2 = \int_0^r \left(\frac{r}{\rho_{\infty}} \right) dr^2 = z^2 \quad (A-6)$$

$$\psi = \psi^* \quad (A-7)$$

$$(r \bar{u'v'}) \rho (r dr dx) = (r^* \rho_{\infty} \bar{u'v'}^*) r_{\infty}^* r^* dr^* dx^* \quad (A-8)$$

The last equation leads to

$$\bar{u'v'} r = r^* \rho_{\infty} \bar{u'v'}^* \quad (A-9)$$

The stream functions are related to the velocity components as follows:

$$\rho u r = \rho_{\infty} \psi_r \quad (\rho v + \bar{r'v'}) r = -\rho_{\infty} \psi_x$$

$$\text{and} \quad u^* r^* = \psi_{r^*} \quad v^* r^* = -\psi_{x^*}$$

Equation (A-7) yields

$$u^* = u \text{ and } r(\rho v + \bar{r'v'}) = \rho_{\infty} [r^* v^* - r^* r_{x^*}^* u^*]$$

The continuity and momentum equations for the compressible wake flow (Equations 1 and 2) then become the corresponding equations for incompressible flow:

$$(u^* r^*)_{x^*} + (v^* r^*)_{r^*} = 0 \quad (A-10)$$

and

$$u^* u_{x^*}^* + v^* u_{r^*}^* = \frac{-1}{r^*} (r^* \bar{u'v'}^*)_{r^*} \quad (A-11)$$

If the eddy viscosity is introduced, Equation (A-9) becomes

$$\begin{aligned}
 r \rho \epsilon \frac{\partial u}{\partial r} &= r^* \rho_{\infty} \epsilon^* \frac{\partial u^*}{\partial r^*} \\
 \text{or} \quad \mu_t &= \epsilon = \left(\frac{r^*}{r} \right)^2 \frac{\rho_{\infty}}{\rho} (\rho_{\infty} \epsilon^*) = \frac{\rho_{\infty} \epsilon^*}{\rho r^2} \int_0^{r^2} \bar{\rho} \, d r^2 \quad \left. \vphantom{\frac{\rho_{\infty} \epsilon^*}{\rho r^2}} \right\} \quad (A-12)
 \end{aligned}$$

Along the axis, we have $\mu_t(x, 0) = \rho_{\infty} \epsilon^*$

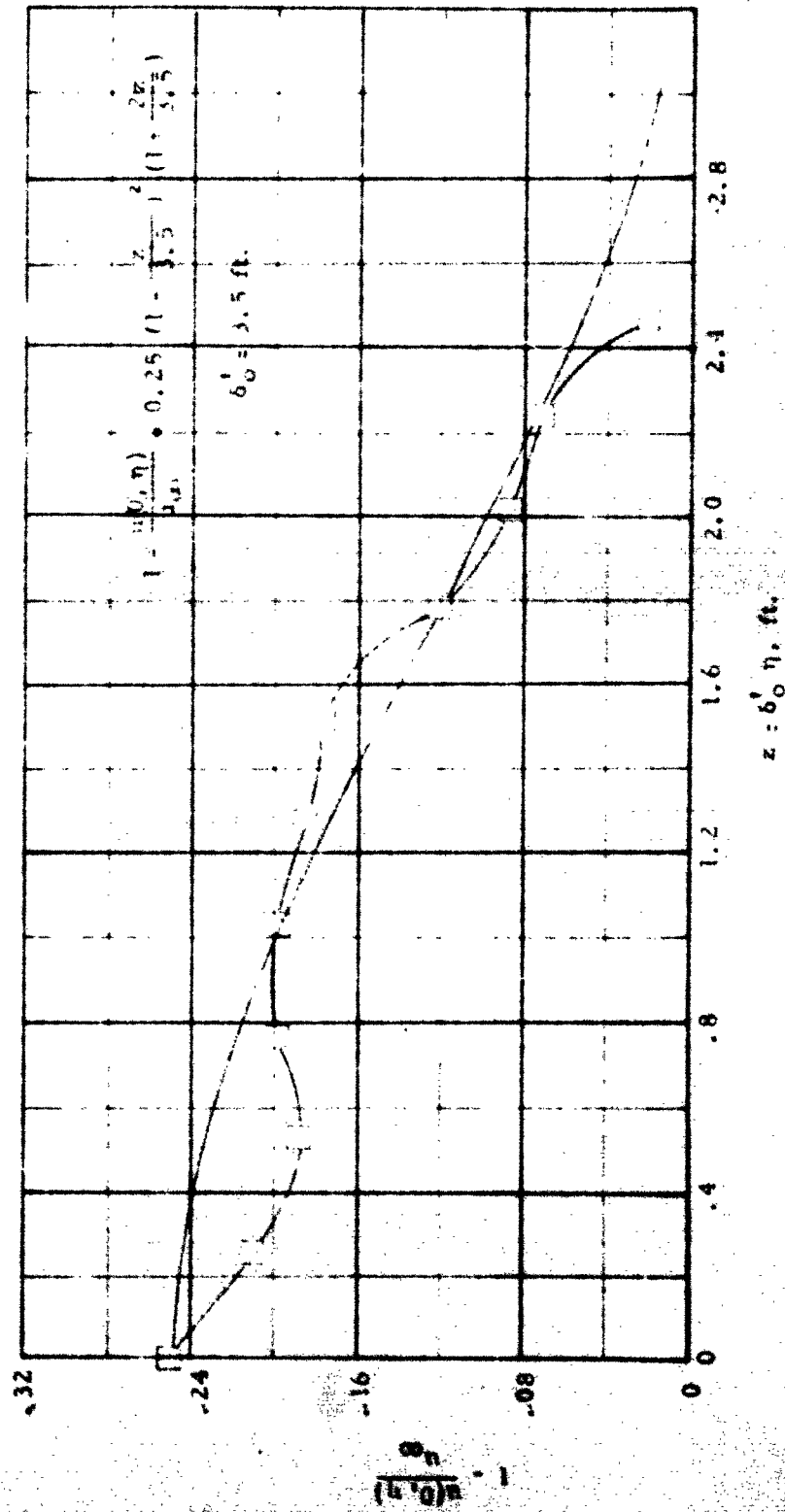


Figure 1 - Initial Velocity Profile for Equilibrium Flow

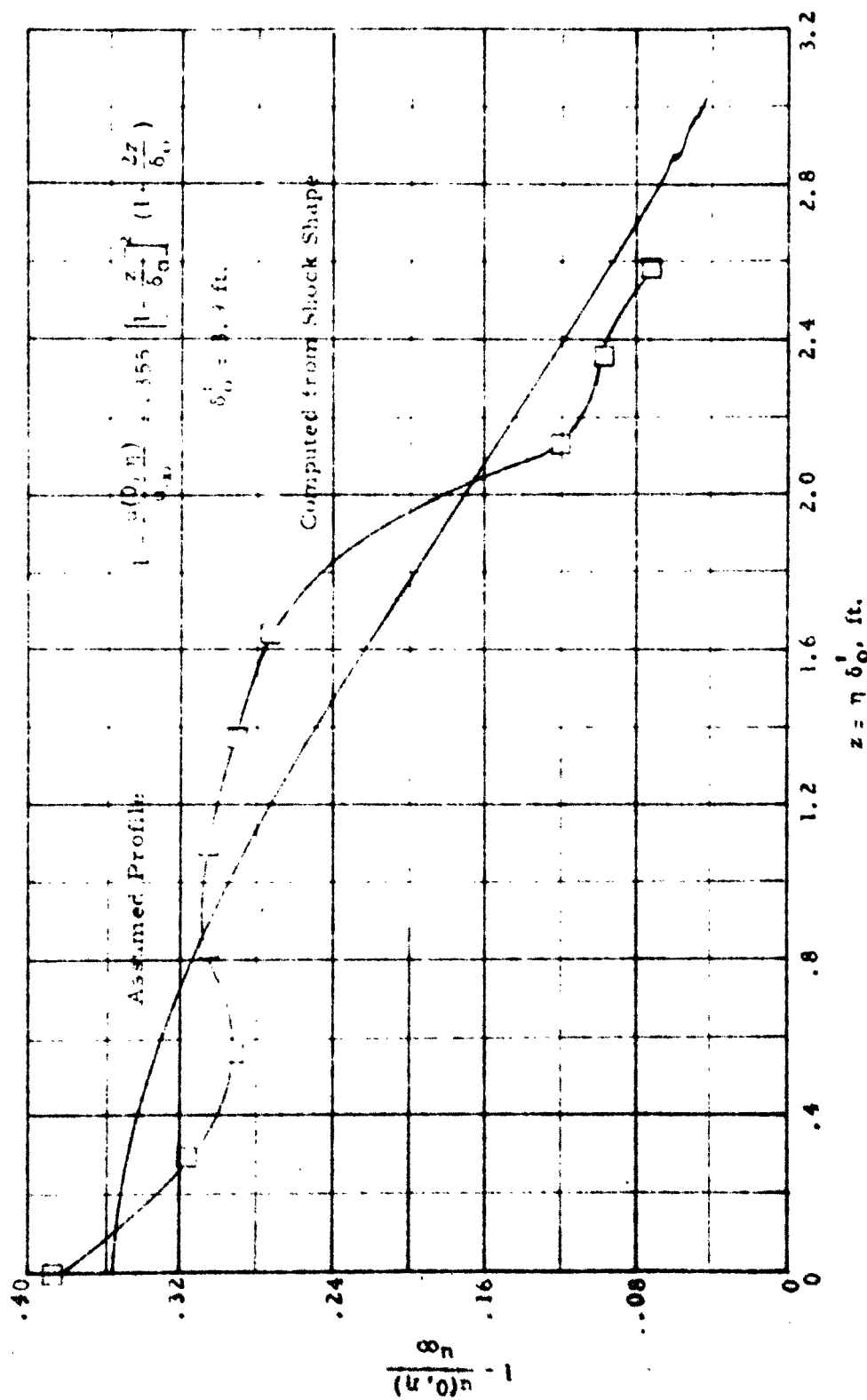


Figure 2 - Initial Velocity Profile for Frozen Flow

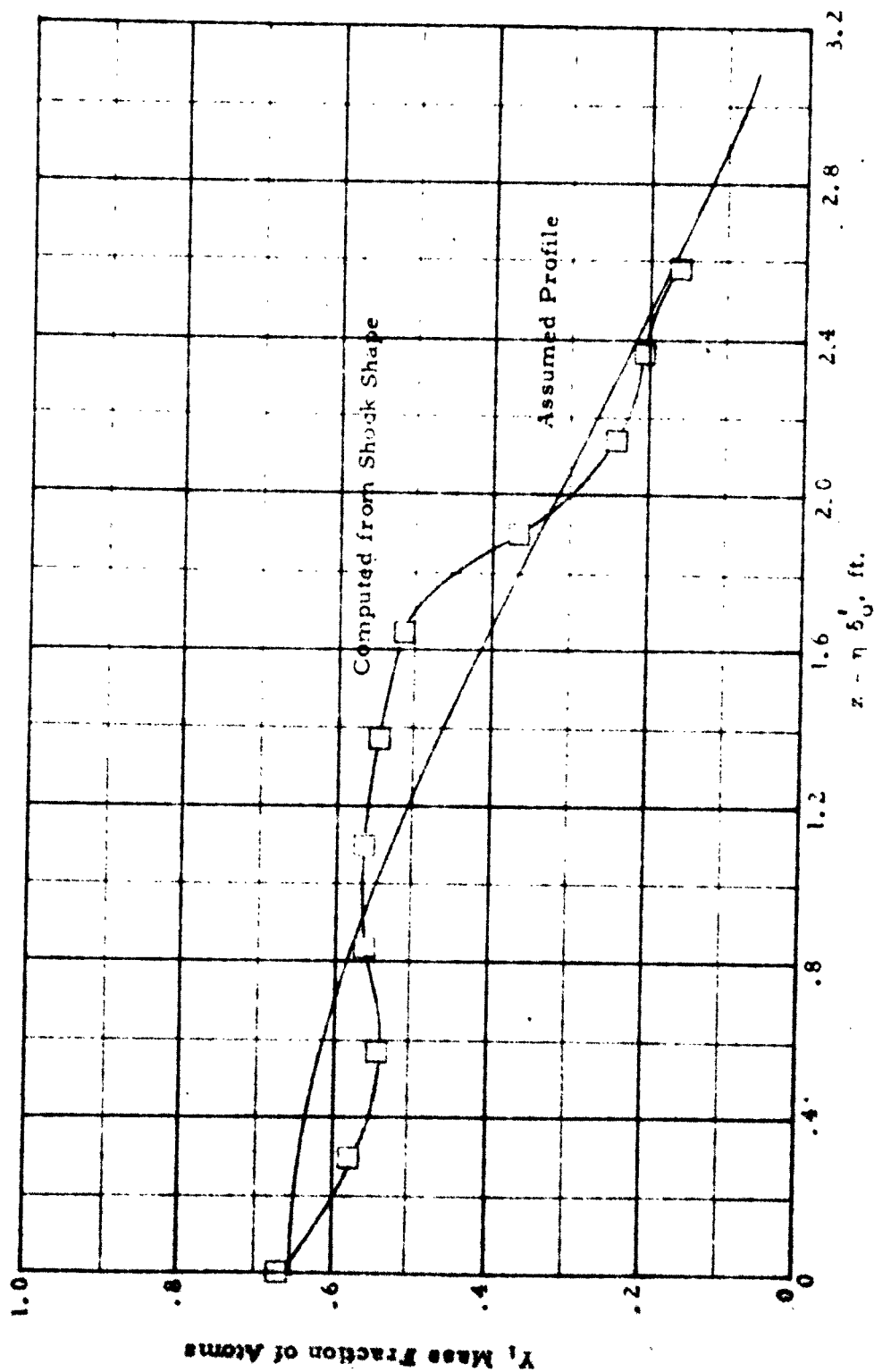


Figure 3 - Initial Mass Fraction of Atoms for Frozen Flow

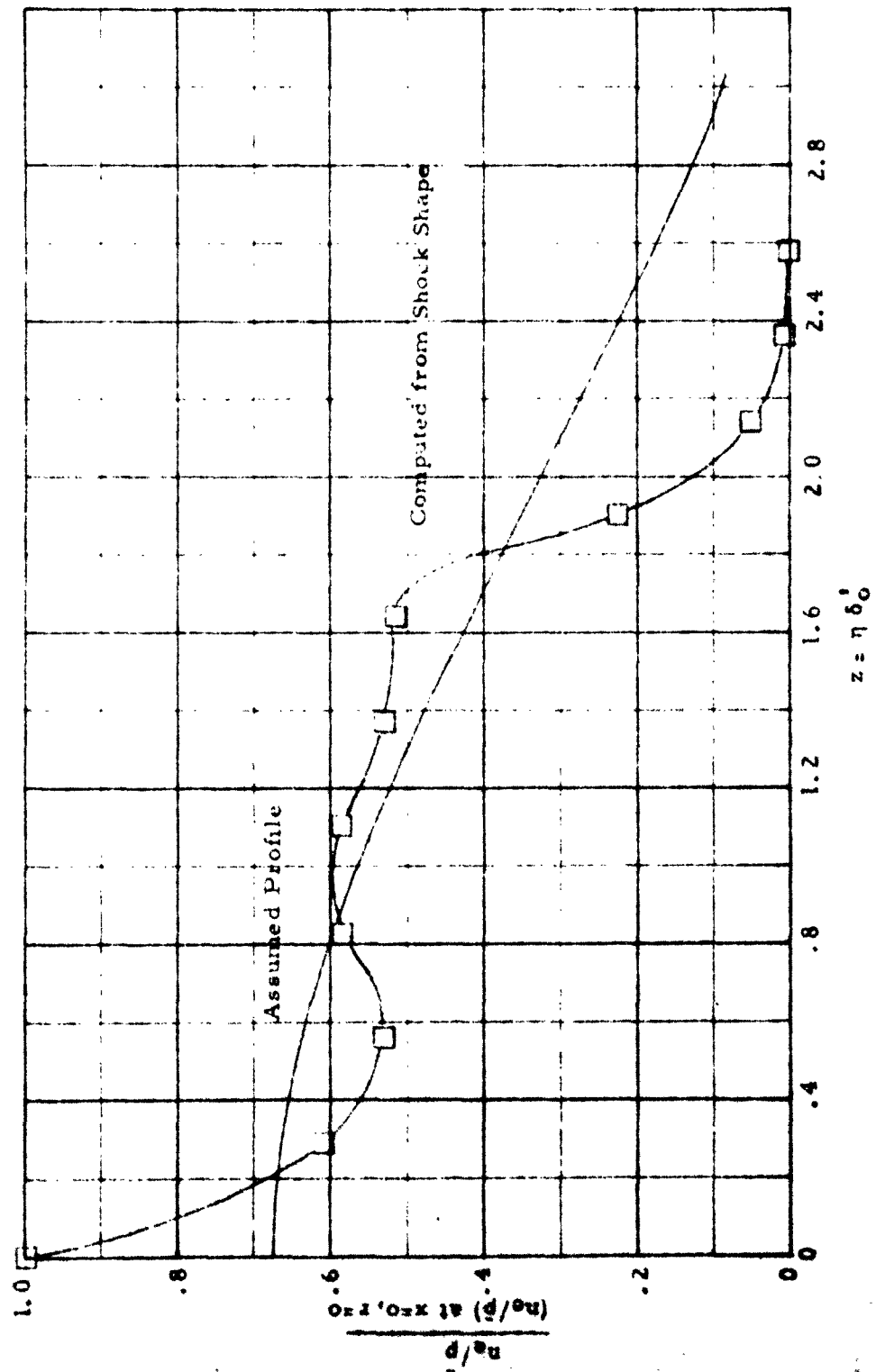
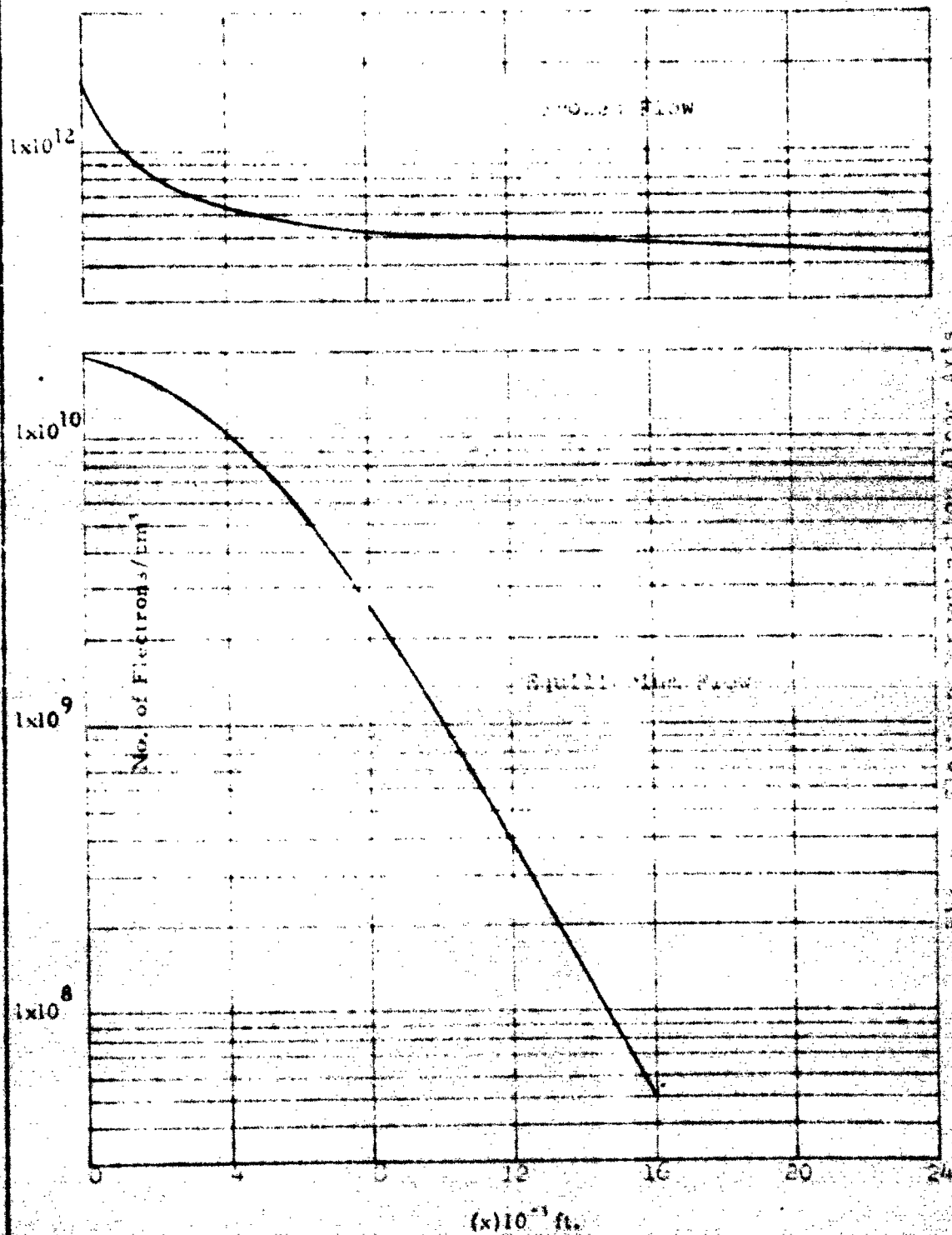


Figure 4 - Initial Profile of Electrons per Unit Mass for Frozen Flow, Initial Data

Fig. 3 - Electron Concentration Along Axis
For the Laminar Flow

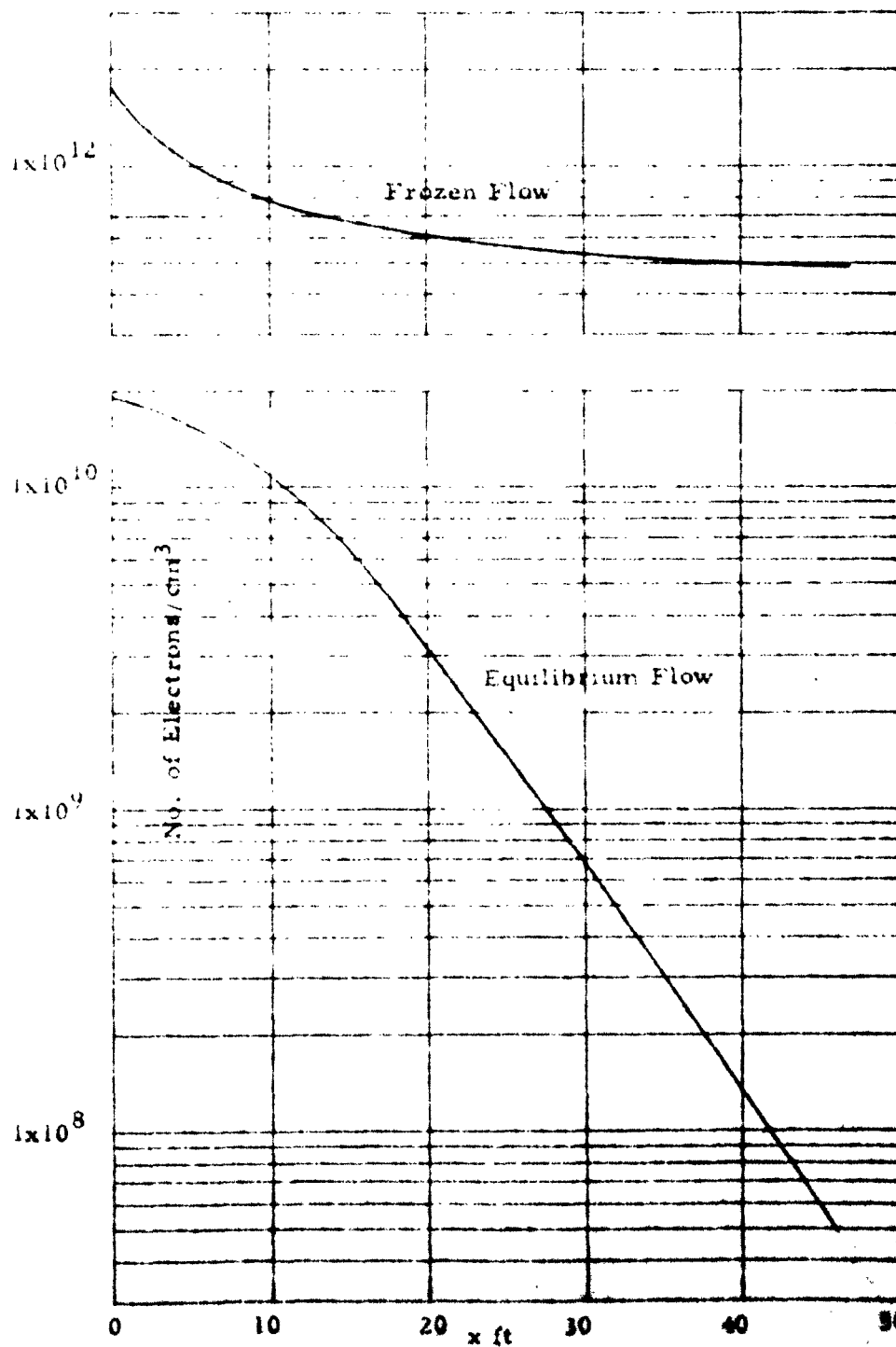


Figure 6 - Electron Concentration Along the Axis
For the Turbulent Wake Flow.

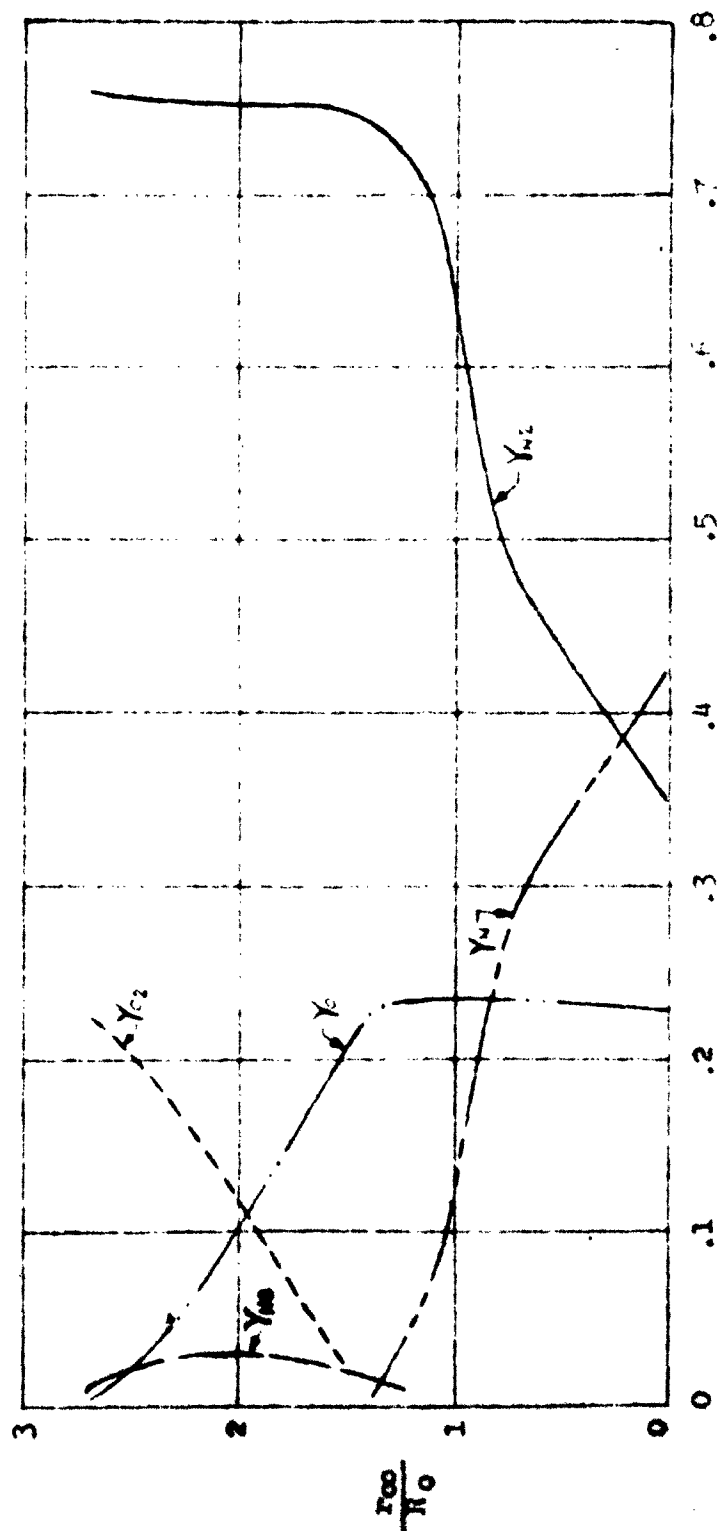


Fig. 7 Radial Distribution of Mass Fraction of Major Constituents Behind Bow Shock

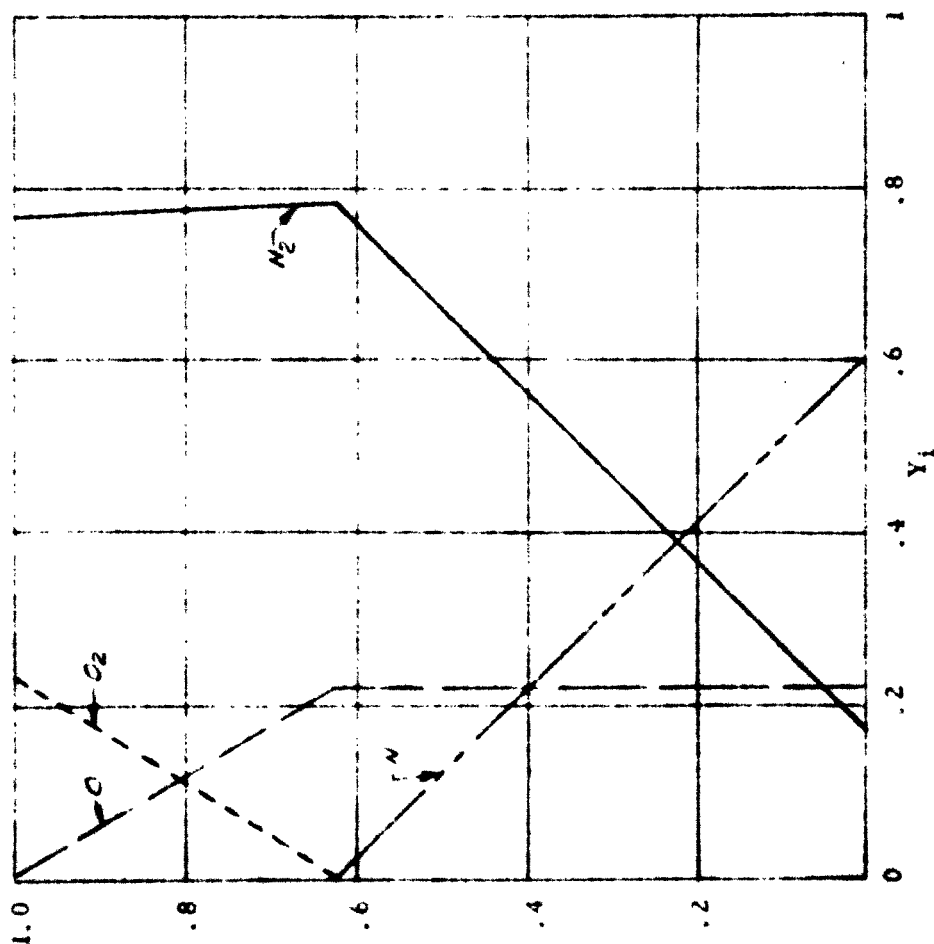


Figure 8 - Mass Fraction Distribution in the Initial Section of the Wake

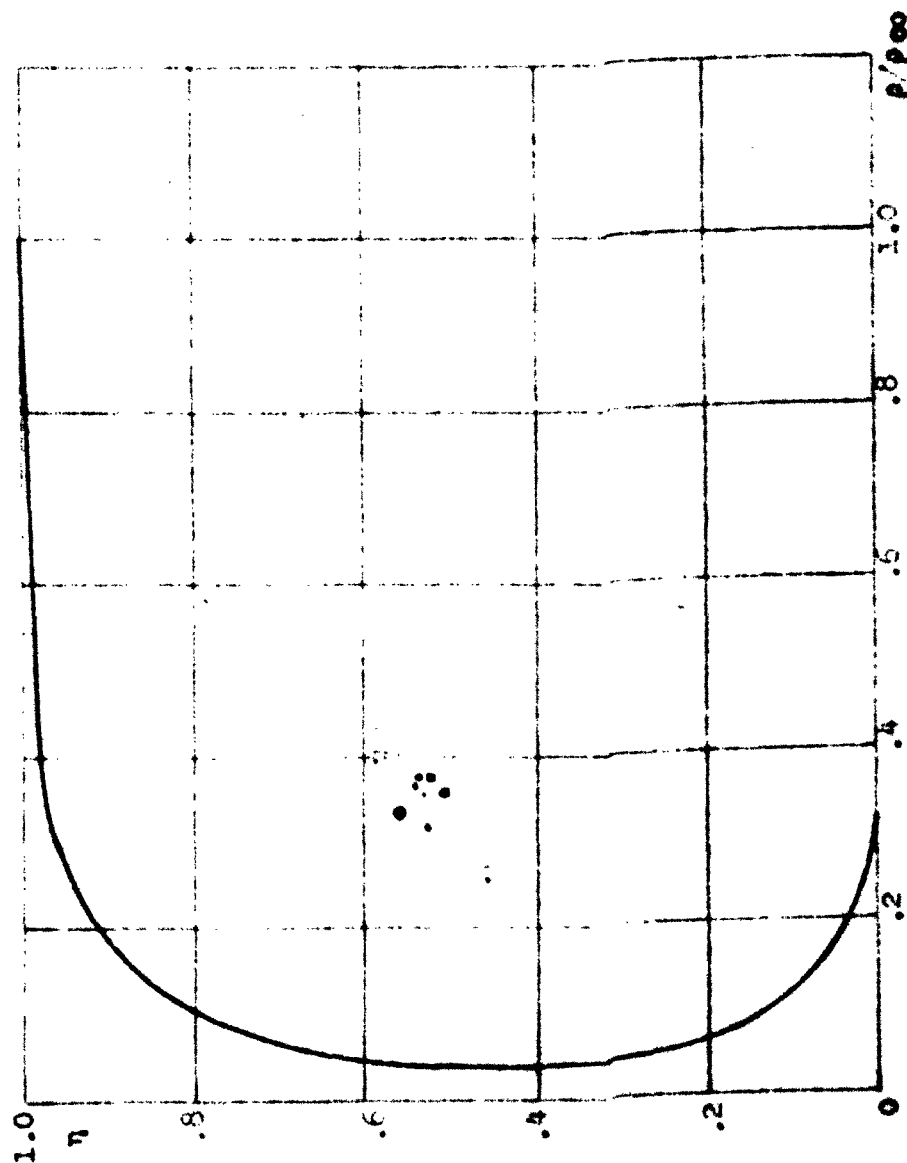


Fig. 9 Density Of The Mixture In The Initial Section
Of The Wake

UNCLASSIFIED

UNCLASSIFIED